Determination of geocenter coordinates and Earth rotation parameters based on Galileo observations

R. Zajdel[1], K. Sośnica[1], G. Bury[1], R. Dach[2], L. Prange[2]

1. Institute of Geodesy and Geoinformatics, WUELS
2. Astronomical Institute, University of Bern
radoslaw.zajdel@igig.up.wroc.pl

EGU General Assembly 2019, 8-12 April, Vienna

WROCŁAW UNIVERSITY OF ENVIRONMENTAL AND LIFE SCIENCES

1. Introduction

The Global Navigational Satellite System (GNSS) is one of the major satellite techniques, which can deliver valuable information about Earth Rotation Parameters (ERPs). The GNSS satellites are also sensitive to the geocenter motion, however, the time series of the GNSS-based geocenter coordinates (GCC) differ to SLR-based products, especially for the Z component. Both ERPs and GCC are vulnerable to the spurious effects, which originate from the orbit modeling issues and GNSS constellation characteristics. The European GNSS Galileo may be considered as fully operational with 24 healthy satellites in space. Unlike the Galileo system, the contribution of GPS and GLONASS systems to the determination of GCC and ERPs has been already discussed in recent years [1]. This contribution shows results of the determination of the Galileo-based ERPs and GCC and a comparison of the results delivered by GPS, GLONASS, and the combined solution. The processing is based on RINEX3 files from the global network of ~100 multi-GNSS stations (Fig.1.1), all of which track GPS, GLONASS and Galileo satellites.
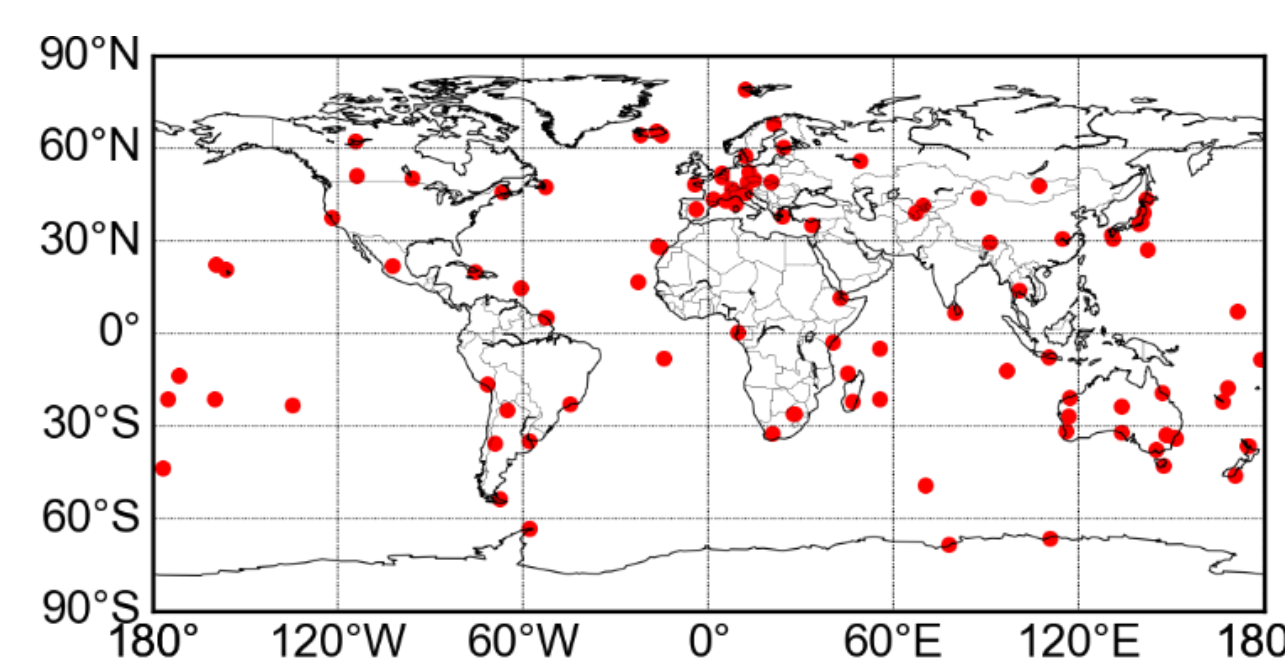

Fig.1.1 Distribution of GNSS stations

2. Methodology

All computations are performed using the latest development version of the Bernese GNSS Software. The vast majority of the settings in the processing strategy is adopted from the CODE's (Center for Orbit Determination in Europe) solution for the IGS's (International GNSS Service) multi-GNSS Pilot Project [2]. The standard one-day solutions are prepared using data from 2017-2018. The station coordinates, troposphere parameters, GCC, ERPs and orbits were estimated, as for the standard IGS processing. We assess the individual impact of the GPS, GLONASS, and Galileo constellation on the GCC and ERP estimates using the global network consisting of the same set of stations in each case and the same approach as Scaramuzza [3]. The computations of system-specific GCC, i.e., estimating GCC separately for GPS, GLONASS, and Galileo, are based on the same normal equation systems (NEQs) as the standard combined solution. Additionally, we compared two approaches of the Solar Radiation Pressure (SRP) modeling in the Galileo orbit solution. First approach assume the empirical ECOM2 [4] model with 7 parameters (3 constant accelerations in DYB directions, sine and cosine one-per-revolution terms in B, sine and cosine twice-per-revolution terms in D. The second approach combines physically BOXWING [5] and empirical ECOM model, reduced to the constant accelerations in DYB directions only (see Table 2.1). We have composed the BOXWING model, based on the Galileo metadata released in late 2017 by the European GNSS Service Centre.

Symbol	Systems	Orbit modelling
GRE	GPS+Galileo+GLONASS	ECOM2 (7 par)
GPS	GPS	ECOM2 (7 par)
GLO	GLONASS	ECOM2 (7 par)
GAL	Galileo	ECOM2 (7 par)
GAB	Galileo	BOXWING & D_0, Y_0, B_0

Table 2.1 Description of the solutions
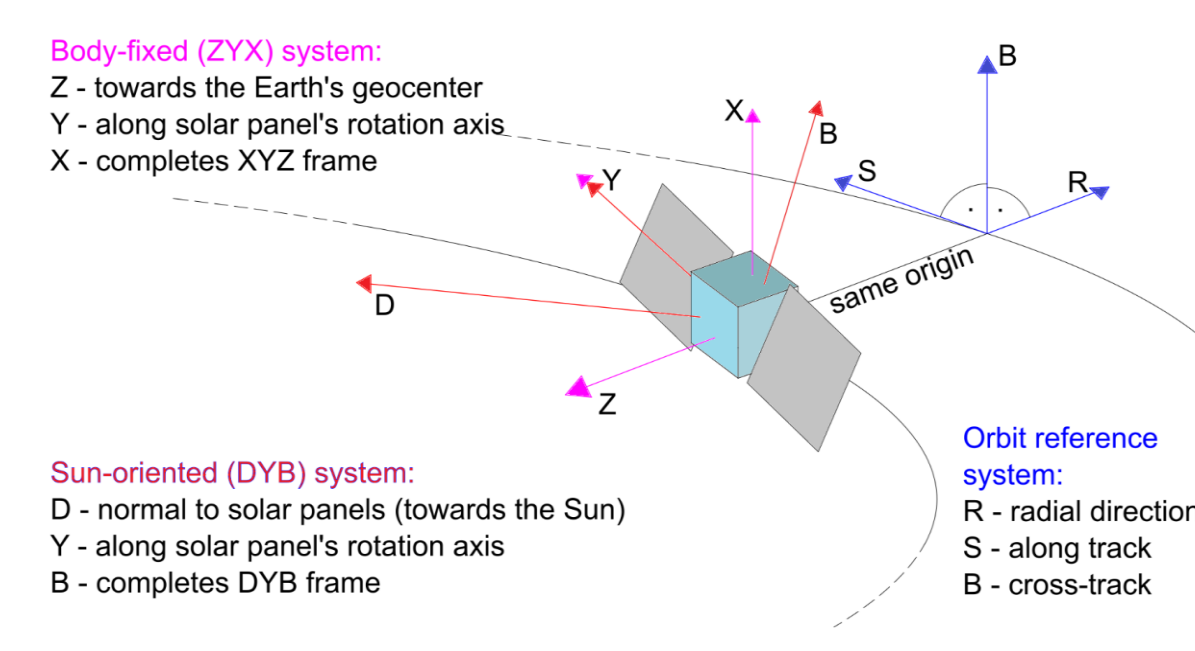
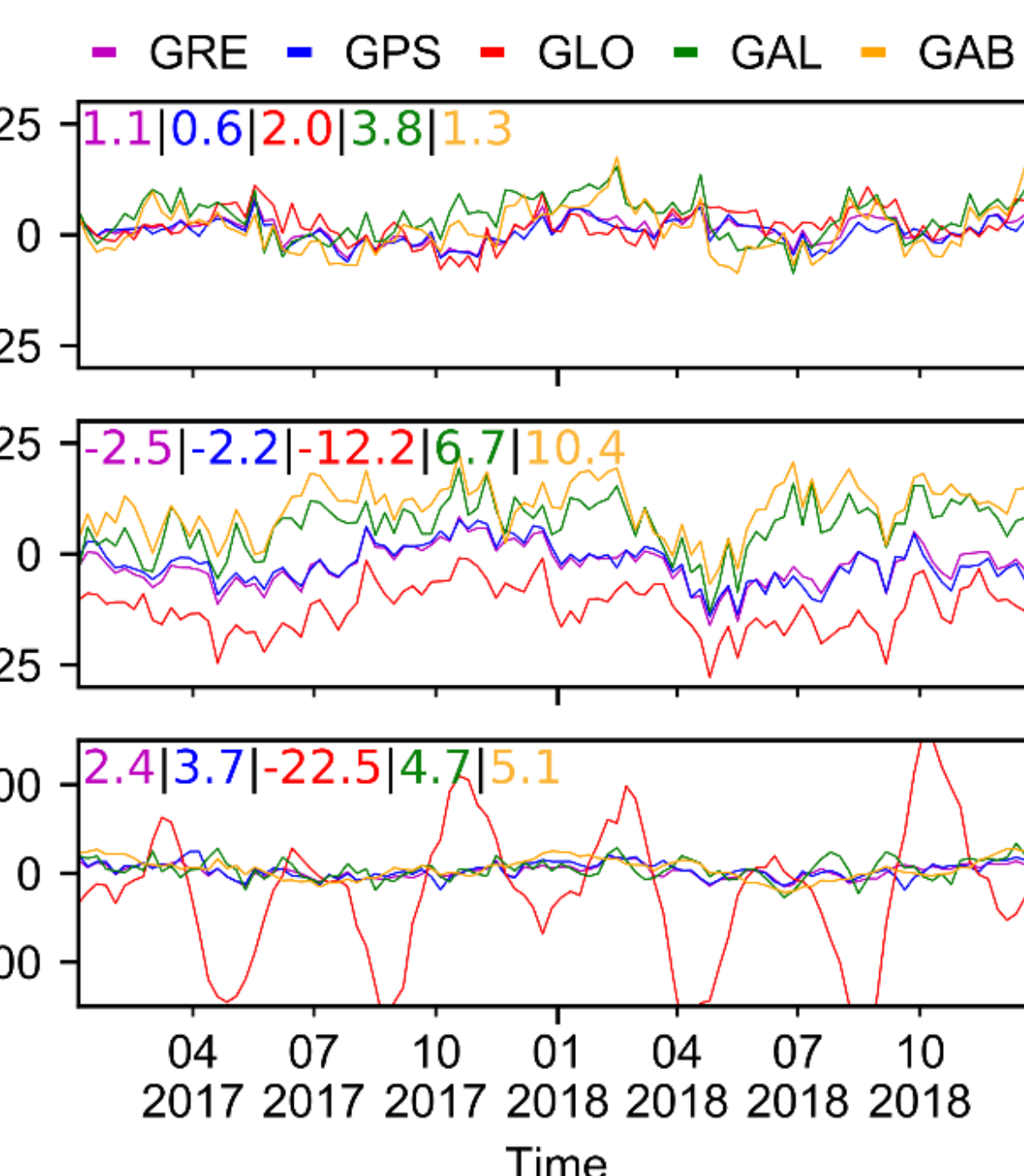Figure 2.1 Orientation of the axes in the satellite-related frames

3. Geocenter coordinates

Fig.3.1 Time series of the geocenter coordinates with mean offsets
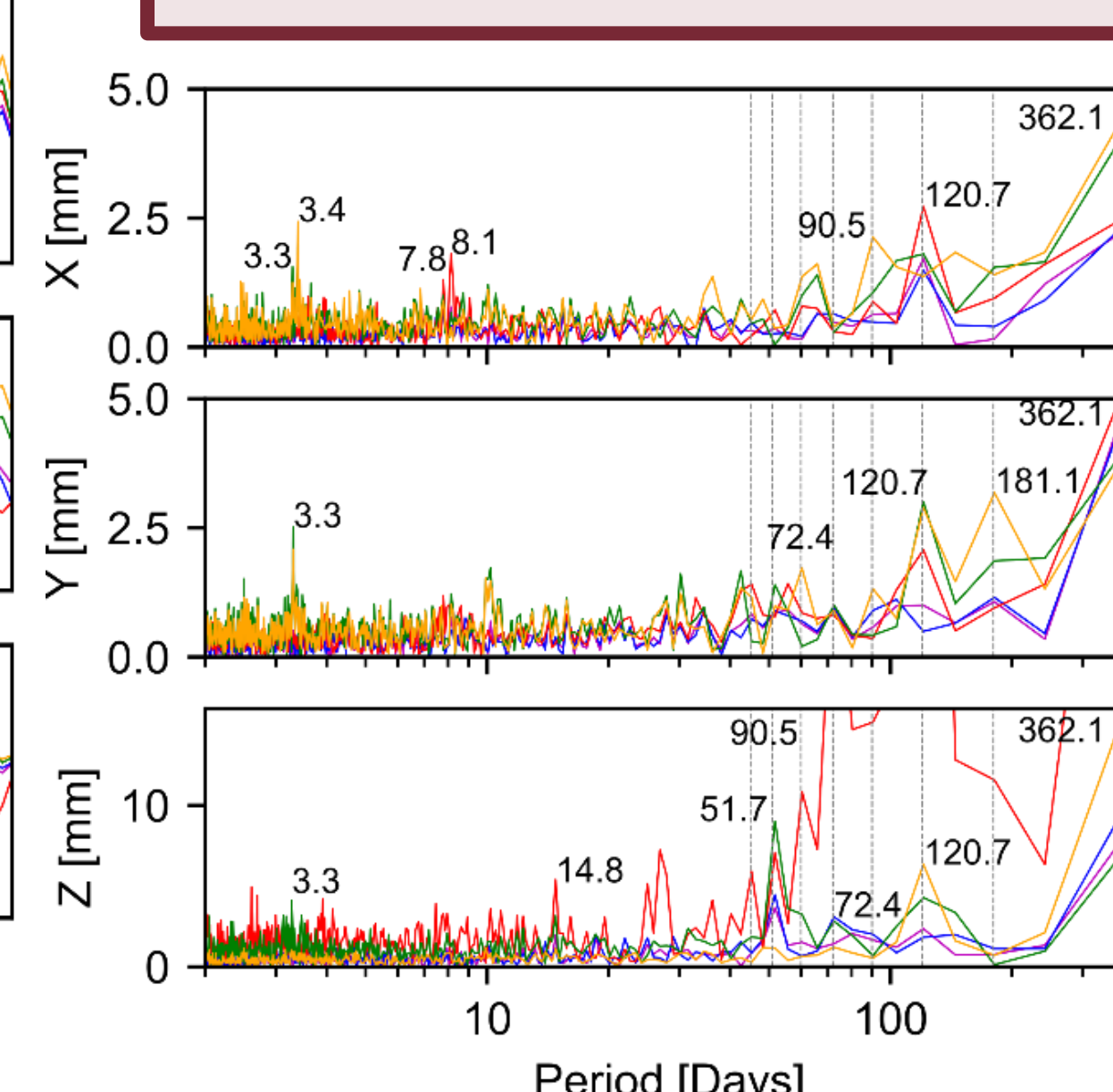

Fig.3.2 Amplitude spectra of the geocenter coordinates

Figures 3.1 and 3.2 illustrate the time series of GCC as well as the amplitude spectra of the signal for the subsequent series. The time series of the horizontal geocenter coordinate are most consistent between different systems. Therefore, all GNSS are sensitive to the same geophysical mass redistribution sensed by the equatorial components of the geocenter. The amplitude of the annual signal equals 4.2, 3.9, 2.4, 2.2 and 2.1 mm in the case of the X component and 3.6, 3.8, 4.8, 4.2 and 4.3 mm in the case of the Y component for GAB, GAL, GLO, GPS, and GRE solutions, respectively. Moreover, the signal with a period close to 3.4 days and the amplitude of ~2.5 mm is visible in the both GAB and GAL series of the X and Y components. The signal is related to the combination of the frequencies of the Galileo revolution period and the arc length [8]. The common period can be described by the equation $T = \frac{T_E \cdot T_S}{T_E - 2T_S}$, where T_E is the Earth rotation period (24h, and the T_S is a satellite revolution period (14.08h). The same effect can be distinguished for GLONASS, while the period of 8.1 days appeared for the X geocenter component with the amplitude of 1.8 mm. The repetition period of Galileo (10 days) is also visible for the Y geocenter component with the amplitude of 1.2 mm. The draconitic signal at 3rd harmonic is dominant for horizontal GCC with the amplitudes of 2.9, 2.9 and 2.1 mm for GAB, GAL and GLO, respectively for the Y component. For the X component, the amplitudes equal 2.7, 1.6 and 1.5 mm for GLO, GRE, and GPS, respectively. The system-specific geocenter coordinate is also systematically shifted depending on the system. The mean offsets equal +7, +10 and -12 mm for GAL, GAB, and GLO, respectively. The 1, 3 and 5 cpy signal with the amplitude of almost 41, 88 and 26 mm is dominant in the time series of the GLONASS-only Z geocenter component. In the case of Galileo, the Z geocenter signal is comparable with that based on GPS. Thus, the spurious nature of the GLONASS series is not caused by the 3-plane configuration of the constellation (as already shown in [1] and [3]). The 7 cpy signal vanishes when using BOXWING. The amplitudes for the 7 cpy signal equal 9.0, 7.0, 4.5 and 3.7 mm, for GAL, GLO, GPS, and GRE solutions, respectively. On the other hand, the annual signal for GAB is 1.7 times larger than for the GPS series.
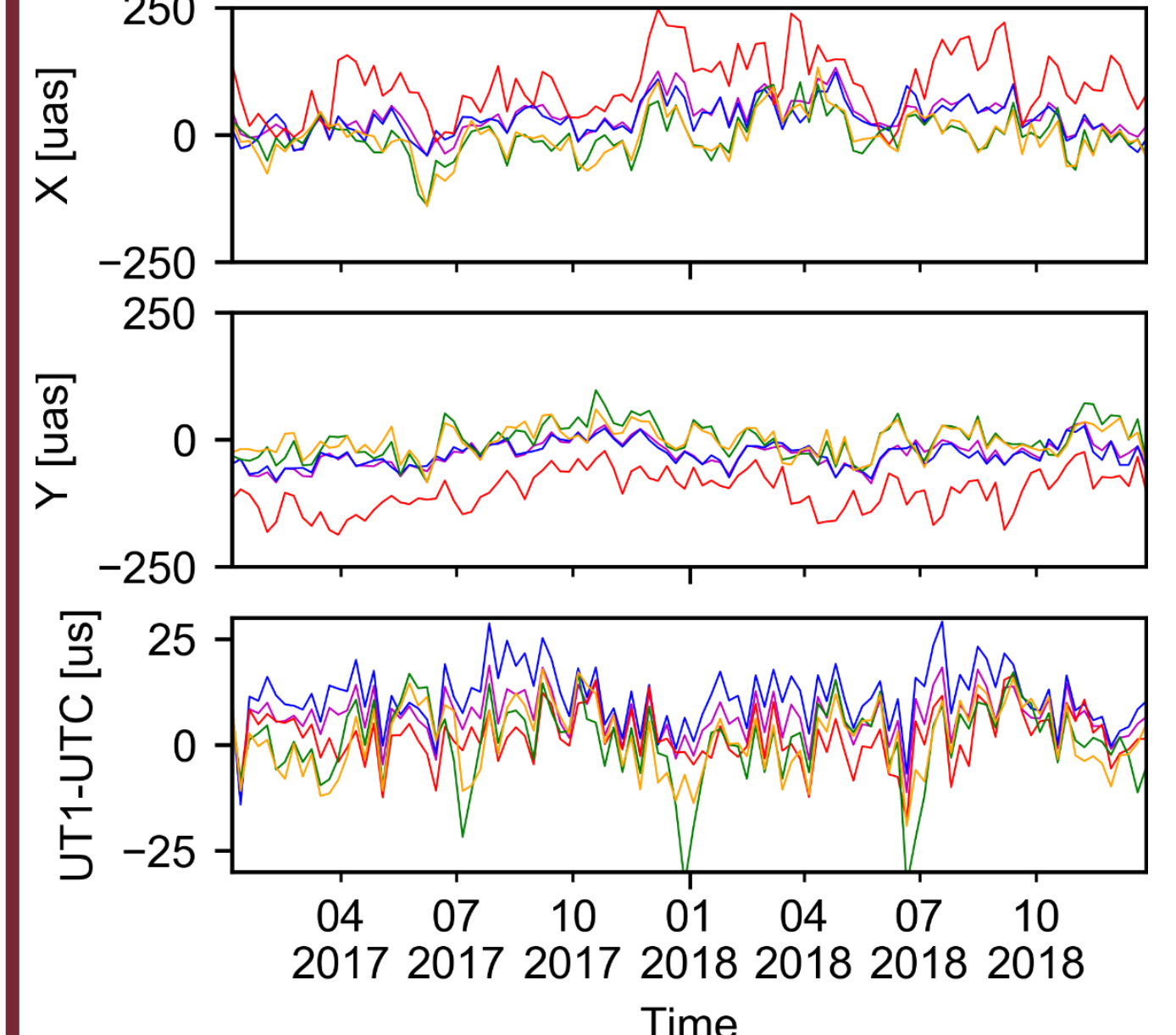
4. Earth Rotation Parameters

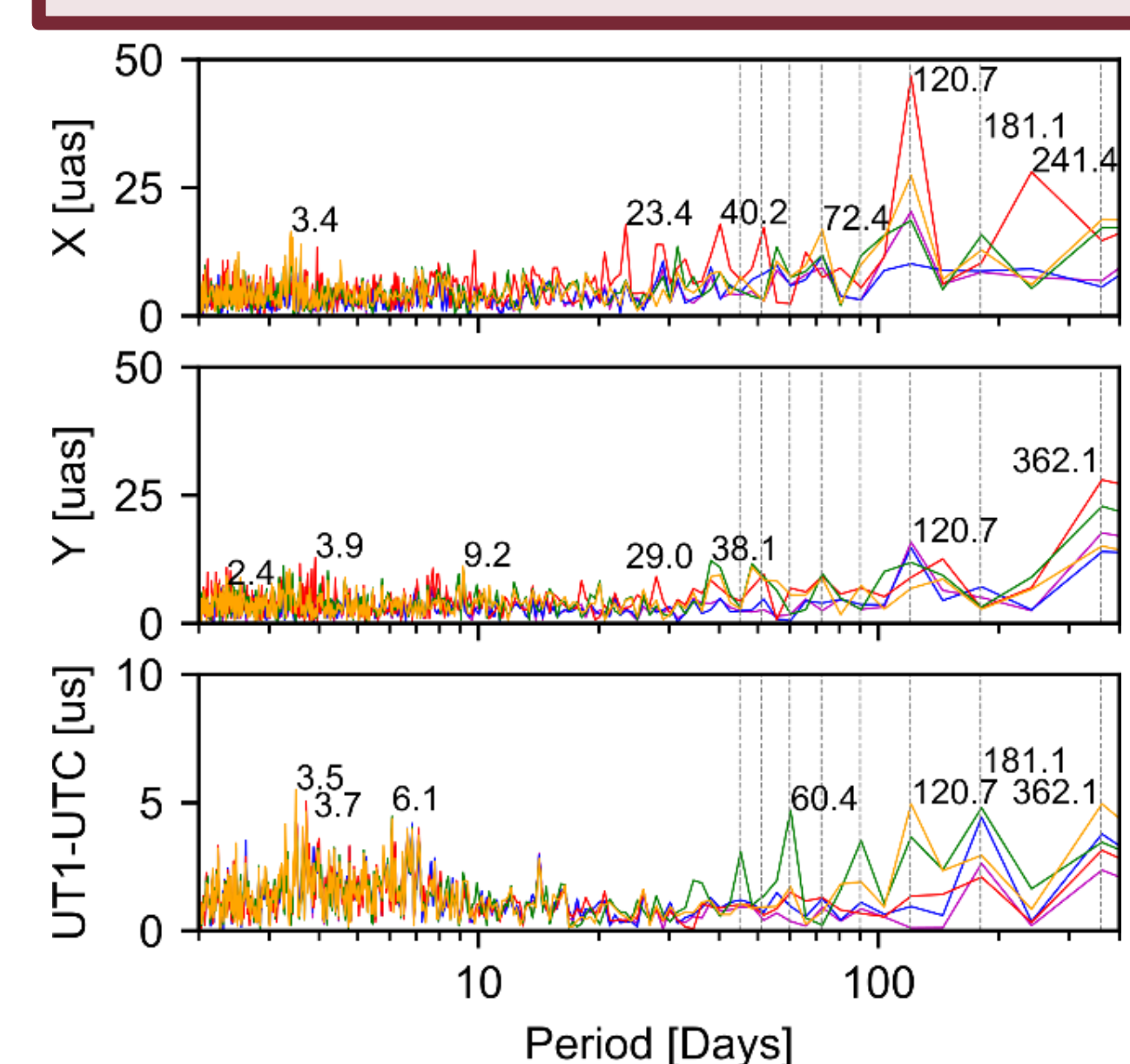Fig.4.1 Time series of ERP differences w.r.t. IERS C04

Fig. 4.2 Spectrum analysis of ERP differences w.r.t. IERS C04

Fig.4.3 Time series of the accumulated UT1-UTC differences w.r.t. IERS C04

Figures 4.1 and 4.2 show the differences of the subsequent series relative to the reference IERS C04 14 values. Table 4.1 shows the systematic biases for the X and Y pole components, which are at the level 30, 100 and 0 µas for GPS, GLONASS, and Galileo, respectively. However, the Galileo-based estimates show larger variability of the values than the GPS and the combined solution, which is expected because the C04 series is dominated by the GPS solutions. The RMS equals 69, 66, 134, 72, 77 for the X pole, 57, 57, 123, 66 and 61 for the Y pole, for GRE, GPS, GLO, GAL and GAB, respectively. Thus, Galileo delivers the ERPs of almost the same quality as the GPS does and much better quality than that from GLONASS. Regarding the comparison of the UT1-UTC results, satellite techniques are not capable to determine the daily rotation of the Earth over a longer period because of the correlation with the drift of the orbital parameter Ω:

$$UT1 \dot{-} UTC = -LOD = -\frac{\dot{\Omega} + \cos(i) \cdot \dot{u}}{k} \quad [6,7,*]. $$ The linear drift of the accumulated UT1-UTC in time is at the level of 8.3 ms/y, which is 1.7 times larger than for the GRE solution and even 5 times larger than for GAL solution (see Fig. 4.3). Moreover, the outliers are clearly visible in the time series of UT1-UTC for GAL and GAB solutions at the epochs which coincide with the largest formal errors (see section 5). The spectral analysis of the X pole coordinate shows the pronounced signal with a 3 cpy period and the amplitude of up to 47 µas for GLO solution. Similarly to the rest of the analyses, the spurious signal with a period close to 3.4 days is discernible for the Galileo-based solutions.
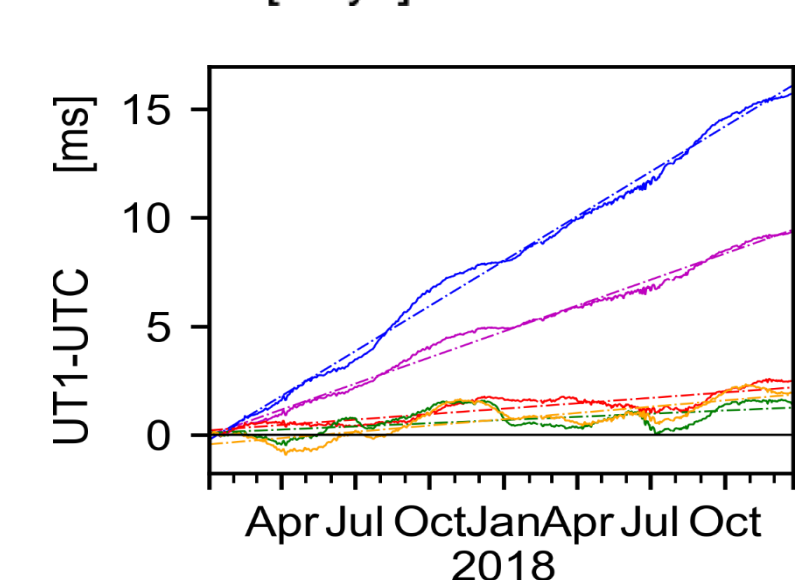
	X [µas]		Y [µas]		dUT1 [µs]	
	AVG	RMS	AVG	RMS	AVG	RMS
GRE	36	69	-27	57	7	22
GPS	31	66	-28	57	11	24
GLO	100	134	-101	123	2	22
GAL	-2	72	-1	66	1	23
GAB	-3	77	-2	61	1	23

Tab.4.1 Mean and standard deviation (STD) of ERP differences w.r.t. IERS C04

[*] Symbols: Ω is a right ascension of the ascending node, i is the inclination, u is the argument of the latitude and k is the ratio of the universal time to sidereal time.
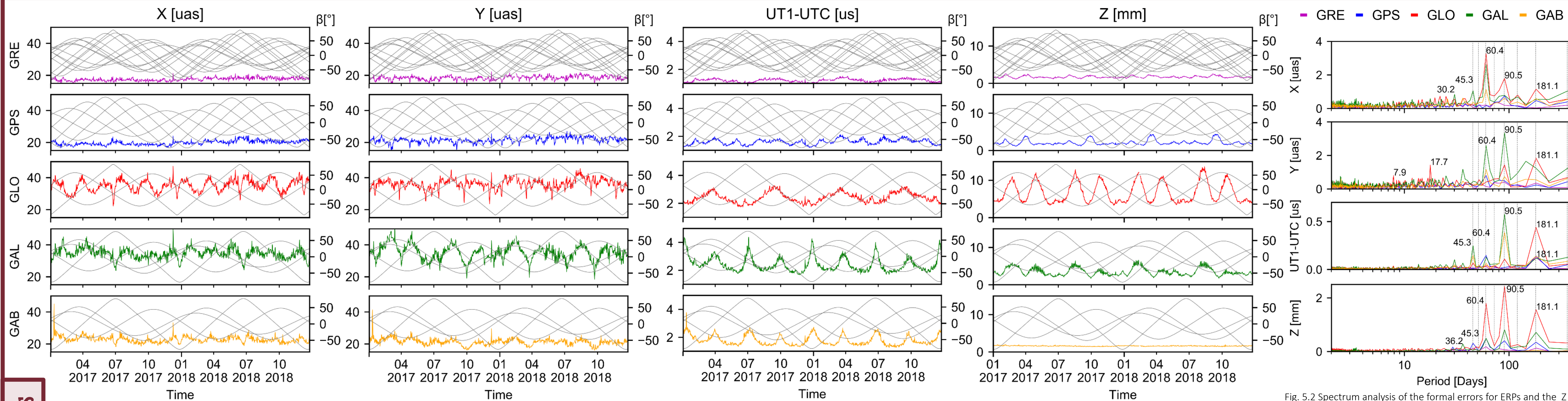
5. Formal errors

Fig. 5.1 Time series of the formal errors for ERPs and the Z component of GCC. Grey lines represent the β angles for the orbital planes of the corresponding GNSS constellations (right axis).

Fig. 5.2 Spectrum analysis of the formal errors for ERPs and the Z component of GCC.

Figure 5.1 shows the formal errors of the ERPs and the Z component of the GCC. A strong correlation is visible between the height of the Sun above the orbital plane (β angle) and the formal errors of the estimated Z component of the GCC. The formal error increases even by a factor of three (from 4 to 12 mm for GLO) when two orbital planes have a similar orientation with respect to the Sun direction. The only exception is a configuration when the similar low values of β for some planes coexist with an extreme value of β for another plane (consistent with [3]). Interestingly, when the hybrid orbit model (BOXWING with estimating constant accelerations) is applied, the periodic variations of the formal errors are entirely reduced. Unlike the GCC, in case of the ERPs, the characteristic patterns are still visible in GAB solution. The parameters have to be partly correlated with the constant accelerations, which are still estimated, especially in the D and X directions (DYB frame [3]). Although both Galileo and GLONASS comprise 3 orbital planes, the periodic variations of the formal errors have a different pattern. In the case of UT1-UTC, the most pronounced signal is visible at the frequencies of 4 cpy and 2 cpy for Galileo and GLONASS, respectively (see Fig 5.2). In case of the Y pole coordinate, the main signal occurs at 2 cpy for GLONASS and at 6 and 4 cpy for Galileo. However, the periodic variation is reduced when cross-referencing GAL with respect to the GAB solution. For the X pole coordinate, the main signal is visible at 6 cpy for both GLO and GAL. Furthermore, the mean error of the parameters is much smaller for the GPS than for the other systems. The formal errors should reflect the mutual contributions of the individual subsystems. Thus, GRE products are mostly influenced by the GPS-based results. The mean errors equal approximately 18,20,35,35,23 µas for the pole coordinates, 1.2, 1.6, 2.4, 2.4, 1.8 µs for the UT1-UTC and 1.7, 2.0, 6.6, 3.5, 1.6 mm for the Z component of the GCC, for GRE, GPS, GLO, GAL and GAB solutions, respectively.

6. ERP and orbit misclosures
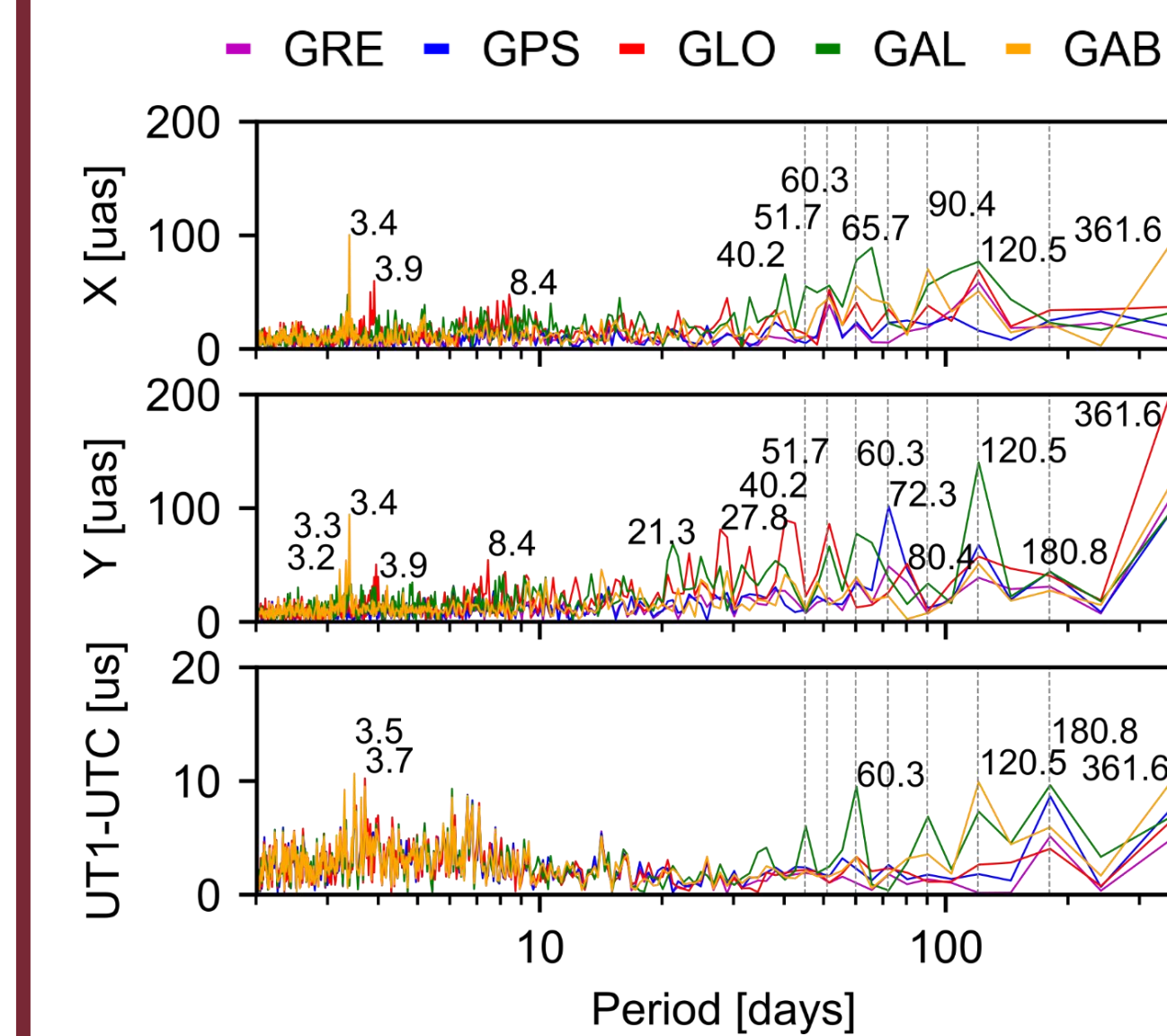

Fig.6.1 Misclosures of the Earth Rotation Parameters
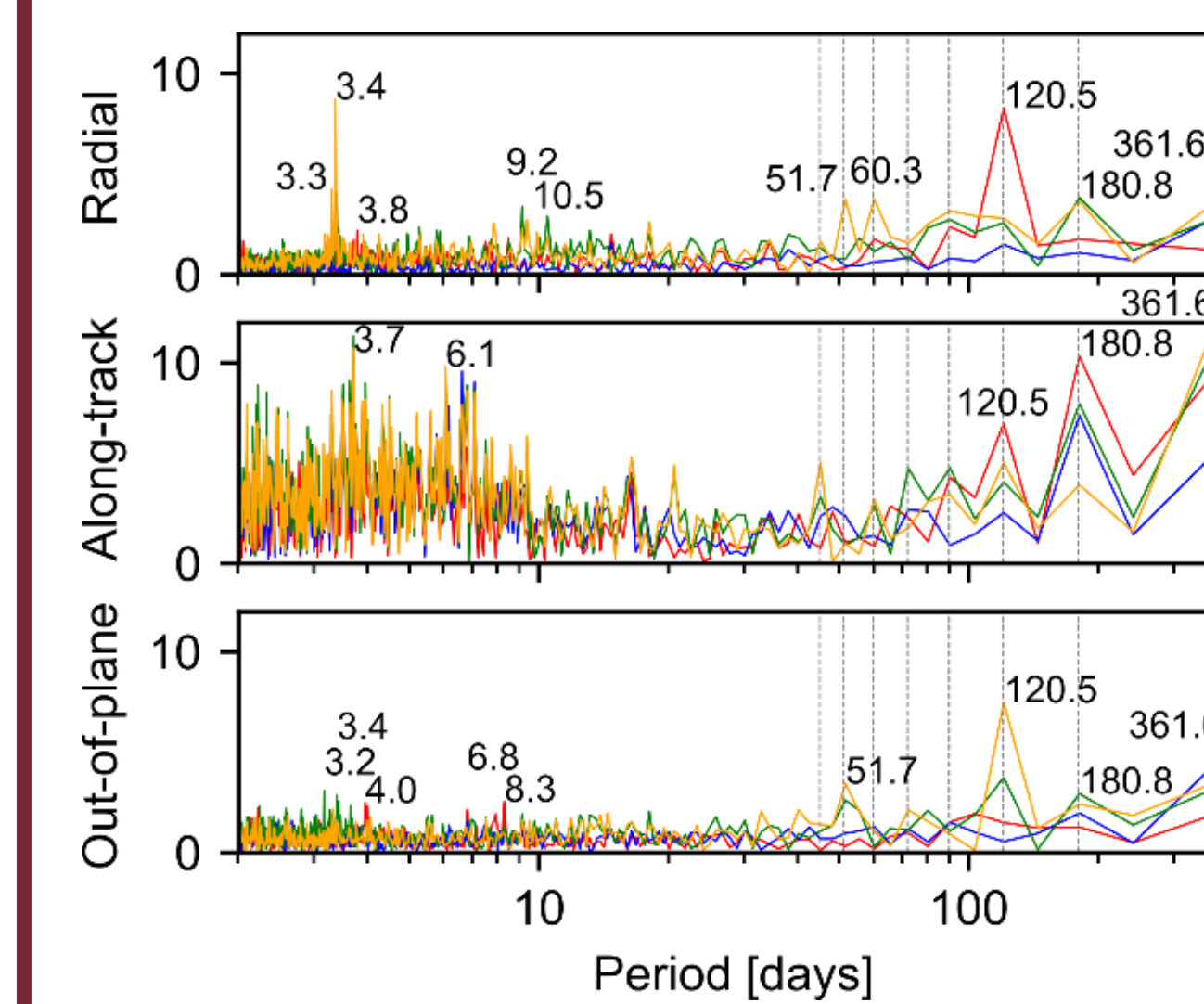
Fig.6.2 Spectrum analysis of the orbit misclosures in the inertial frame

Fig.6.4 Spectrum analysis of the differences between the orbit misclosures in the inertial frame and the orbit misclosures in the Earth-fixed frame

Fig.6.3 Boxplots of the ERP misclosures. The description of the box includes the median value (above) as well as as first (left-below) and third quartile (right-below)

The ERPs are estimated in the 24h interval using a piece-wise linear parameterization. The estimates are delivered for two subsequent midnight epochs. Thus, it is possible to calculate a misclosure of the ERPs as an indicator of the solution consistency. In all the cases, GRE solution is most consistent, therefore one can conclude that combining many systems in the solution eliminates the system-specific errors. Using hybrid SRP modeling improves the pole misclosures when compared to the standard ECOM2 solution for Galileo. The inter-quartile-range decreases by 12 and 21% for the X and Y coordinate of the pole, respectively. The spectral analysis of the ERP misclosures (see Fig. 6.1) shows a signal with a period close to ~3.3-3.4 days for all ERPs in both GAL and GAB solution. Moreover, in the case of UT1-UTC, the signal with the amplitude of 5-10 µs is visible at 1/8, 1/6, 1/4, 1/3, 1/2 cpy periods for the GAL solution. This pattern is mostly mitigated for the GAB solution. Each system shows the periodic signal for the misclosures of the Y pole coordinate. The annual signal for GLONASS reaches the amplitude of 200 µas and is almost twice as large as for the other systems. The 3 cpy for GAL solution is also twice as large as for the other systems and reaches the amplitude of 130 µas. The largest peak for the GPS system appears for the period of 5 cpy with the amplitude of 96 µas. Most of the harmonic period for GAL solution disappear when using the hybrid model for SRP modeling. Orbit misclosures may be calculated in the inertial or in the Earth-fixed system. Orbit misclosures in the Earth-fixed frame reflect the orbit modelling performance where as in the inertial frame also the ERP misclosures contribute. The difference between both aforementioned methods should outline the impact of the ERP misclosures on the orbits. The largest impact is visible for the along-track component, while the radial direction is roughly unchanged. The largest peaks are visible for the 1 and ½ cpy as well as for the 14.2 and 25.8 days with the amplitude of up to 10 mm.
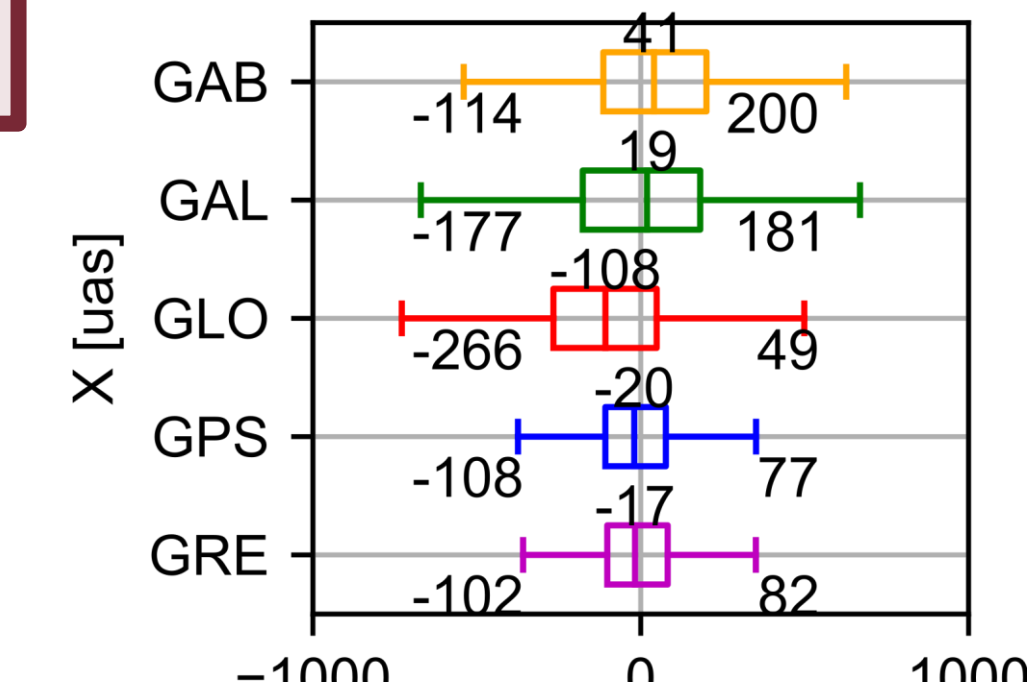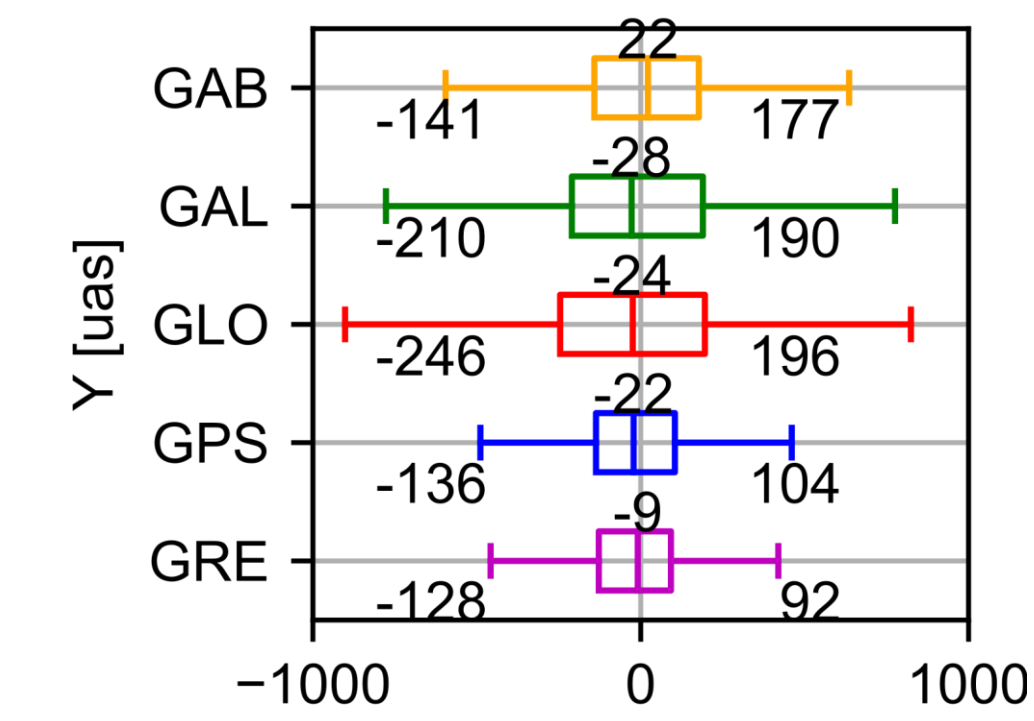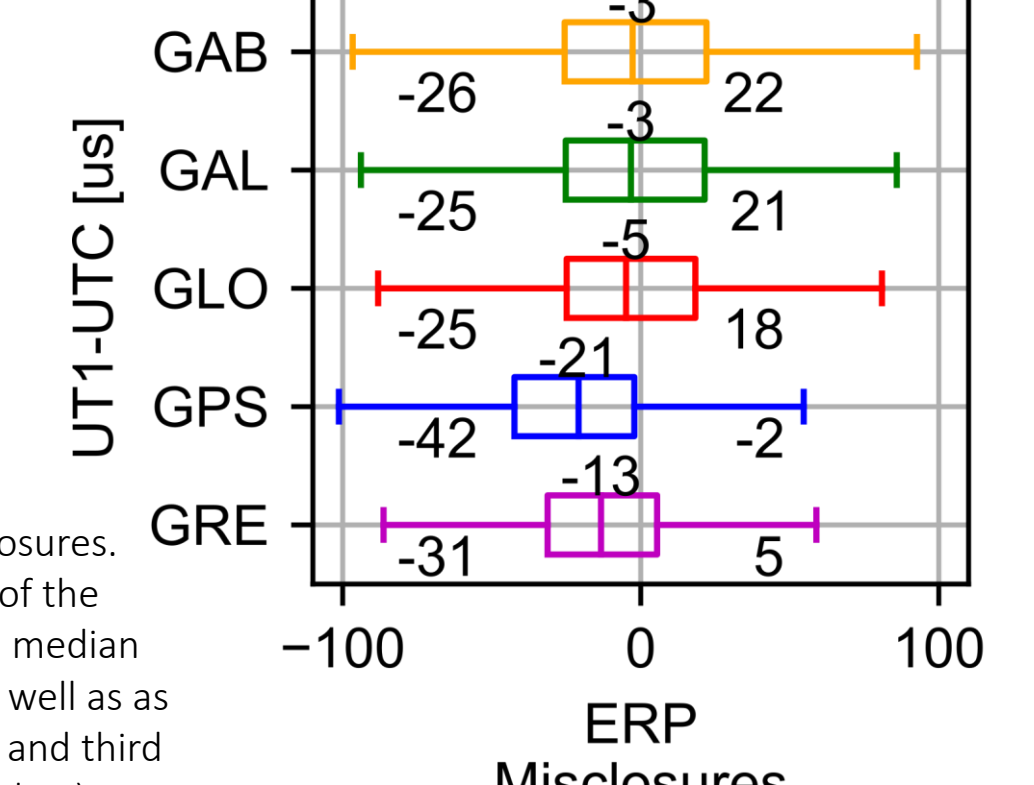
7. Conclusions

- We show that Galileo can deliver geocenter coordinates and Earth Rotation Parameters of the comparable quality to those of the GPS and better quality than GLONASS (see Table 4.1).
- Despite that, both GLONASS and Galileo comprise 3 orbital planes, Galileo is not vulnerable to the same spurious signals as GLONASS is, i.e. the Z-geocenter coordinate, the formal errors of ERPs and ERP misclosures (see Fig. 3.2, Fig. 4.2, Fig. 5.2, Fig. 6.1 and 6.2)
- The artificial signal with a period close to 3.4 days is visible for the majority of the Galileo-derived parameters. We identify this signal as a consequence of the combination of the Galileo revolution period and the solution lengths. The different arc lengths should be further investigated in the next studies to confirm this finding.
- The drift of the UT1-UTC values from the C04 values is 5 times smaller for the Galileo than for GPS. According to [9], this might be related to the arc length.
- Using hybrid SRP modeling, which includes both physical BOXWING model and empirical constant accelerations in DYB directions, reduces the artificial signals in the time series of the Galileo-based parameters.

[1] Meindl, M.; 2011: Combined Analysis of Observations from Different Global Navigation Satellite Systems. Geodätisch-geophysik. Arbeiten in der Schweiz, vol. 83
[2] Prange, L. et al.; 2016: CODE's five-system orbit and clock solution - the challenges of multi-GNSS data analysis. Journal of Geodesy, pp. 345-360. DOI 10.1007/s00190-016-0968-8;
[3] Scaramuzza, S. et al.; 2017: Dependency of geodynamic parameters on the GNSS constellation. Journal of Geodesy, pp 93-104 DOI 10.1007/s00190-017-1047-5
[4] Arnold, D. et al.; 2015: CODE's new solar radiation pressure model for GNSS orbit determination. Journal of Geodesy, pp. 775-791. DOI 10.1007/s00190-015-0814-4
[5] Bury G., Zajdel R., Sośnica K.; 2019: Perturbing forces acing on the Galileo satellites; (under review)
[6] Thaller, D.; 2008: Inter-technique combination based on homogeneous normal equation systems including station coordinates, Earth orientation and troposphere parameters. Scientific Technical Report STR 08/15, Deutsches GeoForschungsZentrum Potsdam, ISSN 1610-0956
[7] Rothacher, M. et al.; 1999: Estimation of nutation using the Global Positioning System. JGR Solid Earth, DOI 10.1029/1998JB900078
[8] Stewart, M. et al.; 2005: Investigating the propagation mechanism of unmodelled systematic errors on coordinate time series estimated using least squares; Journal of Geodesy; pp 479–489. DOI 10.1007/s00190-005-0478-6
[9] Lutz, S. et al.; 2016: Impact of the arc length on GNSS analysis results; Journal of Geodesy; pp. 365-378. DOI: 10.1007/s00190-015-0878-1